Journal of Sound and Vibration 326 (2009) 503–521

Contents lists available at ScienceDirect

Journal of Sound and Vibration

journal homepage: www.elsevier.com/locate/jsvi

An innovative isolation bearing for motion-sensitive equipment

M. Ismail, J. Rodellar *, F. Ikhouane

Department of Applied Mathematics III, Control, Dynamics and Application Laboratory, School of Civil Engineering, Technical University of Catalonia, Campus Nord, Module C-2, 08034-Barcelona, Spain

ARTICLE INFO

Article history:
Received 3 December 2008
Received in revised form
12 June 2009
Accepted 23 June 2009
Handling Editor: C.L. Morfey
Available online 17 July 2009

ABSTRACT

Seismic isolation can protect delicate equipment housed in structures under earthquake attacks. One of the common approaches to isolate equipments is by using isolated secondary raised floors on which the equipments are mounted. This paper presents a new rolling-based seismic isolation bearing, referred to as roll-n-cage (RNC) isolator, for motion-sensitive equipment protection using the raised-floor approach. The RNC isolator is described, modeled and characterized. The effectiveness of the RNC isolator is numerically assessed considering the case of equipment housed in upper floors of a building, where the accelerations are amplified and the motion contains strong components at long periods. The numerical results reveal that the proposed RNC isolator device can attenuate seismic responses effectively under different ground motion excitations while exhibiting robust performance for a wide range of structure–equipment systems.

1. Introduction

Seismic isolation is presently established as the most effective way to mitigate the vibrational response of sensitive equipment housed in structures under earthquake attacks [1,2]. This is particularly important in critical facilities as hospitals, emergency centers, communication and data centers as well as museums. In general, there are three approaches to isolate sensitive equipment [3]: (1) isolation of the entire housing structure, (2) isolation of a single equipment, and (3) isolation of raised-floor systems. The first approach is most appropriate for new construction. Isolators are installed between the structure and its foundation with the objective of reducing the damage of both the primary structure and its contents [4]. The second approach appeared even before the application of seismic isolation in buildings. However, it is usually confronted with a number of problems including the extreme difficulty of achieving the desired long period while keeping affordable displacement and ensuring enough vertical stiffness to support the equipment itself [5,6].

As for the third approach, the sensitive equipment is mounted on a secondary raised floor, which is attempted to be decoupled from the building floor by means of isolation systems. This approach is valid for new construction and retrofitting as well. It has the potential of offering the best of the first approach with lower cost while avoiding the main drawbacks of the second one. Therefore, isolated raised-floor systems are now well established as an effective technique for mitigation of the seismic risk posed on equipments. This is the approach considered in this paper.

A variety of passive, active, semi-active and hybrid isolation systems has been proposed in the literature. Commonly, equipment passive isolation systems are of a sliding-based or rolling-based type [7,8]. Flat sliding bearings are the simplest form of sliding-based devices, but they lack buffer and efficient re-centering mechanisms. They were used for equipment

* Corresponding author. Tel.: +34 93 401 68 65; fax: +34 93 401 18 25.
E-mail addresses: mohammed.ismail@upc.edu (M. Ismail), jose.rodellar@upc.edu (J. Rodellar), faycal.ikhouane@upc.edu (F. Ikhouane).

0022-460X/$ - see front matter © 2009 Elsevier Ltd. All rights reserved.
doi:10.1016/j.jsv.2009.06.022

Nomenclature

c_1	the damping of the first floor
c_e	the damping of equipment
$\mathbf{C}$	the damping matrix of the superstructure
E	the energy quantity
f	the structural natural frequency
F_b	the hysteretic restoring force of Bouc–Wen model
k_1	the stiffness of the first floor
k_e	the stiffness of equipment
$\mathbf{K}$	the stiffness matrix of the superstructure
m_b	the base mass
m_r	the raised-floor mass
$\mathbf{M}$	the mass matrix of the superstructure
n	a parameter of Bouc–Wen model
$\mathbf{r}$	the vector of influence coefficients
t	the time
T	the duration, or structural period
w	an auxiliary variable of Bouc–Wen model
$\ddot{x}_b$	the base mass acceleration
x_e	the displacement at the CG of equipment
$\dot{x}_e$	the velocity at the CG of equipment
$\ddot{x}_f$	the mounting floor acceleration
$\ddot{x}_g$	the ground acceleration
$\ddot{x}_r$	the raised-floor acceleration
$\mathbf{x}_s$	the relative displacement vector of superstructure
$\dot{\mathbf{x}}_s$	the relative velocity vector of superstructure
$\ddot{\mathbf{x}}_s$	the relative acceleration vector of superstructure

Greek letters

ε	the relative error
η	the number of isolators
κ_x	a parameter of Bouc–Wen model
κ_w	a parameter of Bouc–Wen model
ρ	a parameter of Bouc–Wen model
σ	a parameter of Bouc–Wen model

Subscripts

1	L_1 norm, or first floor
∞	L_∞ norm
b	base mass, or the Bouc–Wen model restoring force
e	equipment, or the excitation
f	floor
g	ground
i	variable number, or the input energy
k	kinetic energy
m	measured restoring force from ANSYS
N	number of degrees of freedom
p	potential energy
r	raised floor
s	structure, or the strain energy
y	metallic yield damper
ξ	structural damping

Abbreviations

BIBO	bounded input bounded output
DOF	degree of freedom
FNA	fast nonlinear analysis
FPS	friction pendulum system
RNC	proposed roll-n-cage isolator
SCF	sliding concave foundation
max	special function of maximum value

isolation in [9]. These drawbacks were overcome in [10] through spherically shaped sliding plates in a so-called friction pendulum system (FPS) but on account of equipment uplift. In [6], comprehensive shake table tests were performed on FPS-isolated raised-floor systems used in computer centers. However, FPS tend not to be cost effective for light mass systems. Indeed, regardless of the vertical weight, the displacement is the same for a given effective period and so the size of the slide plates, which are the most expensive part of sliding bearings, is the same for heavy or light mass systems. Another sliding approach, named sliding concave foundation (SCF) system, was presented in [11] and investigated analytically in [3] when used as the isolation device for raised-floor systems. However, it may cause permanent tilting of the isolated object.

Rolling-based bearings offer the maximum equipment-base horizontal decoupling, but they lack damping, buffer and re-centering mechanisms [12–14]. Ref. [15] benefited from the elliptical shape of rollers to ensure a gravity-based re-centering mechanism. However, this shape causes equipment uplift and cannot prevent permanent equipment dislocation under strong earthquakes. To overcome this difficulty, spherical rollers inside two opposite concave plates are proposed in [16] as a rolling-pendulum system. This provides a gravity restoring force without permanent displacement but damping is still missing and uplift is exhibited.

Sliding-pendulum and rolling-pendulum systems provide a natural period of 2–4 s [17]. This period range is not sufficient for effective isolation of light mass systems, as low masses must be associated with low stiffness to achieve the required isolation period [18,5,6]. Moreover, based on their principle of operation, these systems force the isolated object to oscillate as a simple pendulum with a fixed vibration period, which represents a severe practical difficulty of aseismic design. In other words, these isolation systems employ a relatively fixed geometry, which makes the isolator not suitable for a wide range of structure and ground motion characteristics [19]. Some recent studies tried to enhance the adaptability of FPS [19–21].

Alternatively to passive isolation systems, [22–25] explored the possibility of using a hybrid platform to protect equipment from seismic damage. In [26,17,27], the performance and reliability of semi-active equipment isolation was

examined. A smart isolation system that combines an isolation platform with a variable friction device is proposed in [2]. This class of systems are appealing and have a good potential for isolation, but they require sensors and actuators with feedback control loops, which make them more complex than purely passive systems. While research on smart controlled systems is developing, passive isolation systems may be still improvable to offer higher performance keeping design and implementation simplicity in comparison with active or semi-active systems.

In this paper, an innovative seismic isolation bearing, called roll-n-cage (RNC) isolator, is presented for sensitive equipment protection, using the raised-floor approach. It is an attempt to integrate several passive mechanisms into a single unit, in order to overcome the main drawbacks of the present day passive isolators. The RNC isolator is of rolling-based type to offer great horizontal flexibility. Moreover, it is able to resist minor excitations, exhibits no uplift and incorporates damping. It has a built-in re-centering mechanism and buffers for severe earthquakes.

In Section 2, the proposed RNC isolator is briefly described and its principle of operation is explained. Section 3 presents a procedure for the numerical characterization of the RNC isolator using a computer code. A mathematical description of its dynamic behavior is presented in Section 4. Numerical case studies are presented in Section 5 and the corresponding results are given in Section 6 to assess the effectiveness of the RNC isolator.

2. The roll-n-cage isolation system

The roll-n-cage isolation bearing (see Fig. 1) is mainly made up of a stiff rolling body (1) placed between two stiff circular plates (2,3) fixed to the isolated object and the base floor, respectively. The contact between these three parts takes place through less stiff plates (4,5). Metallic yield dampers (6) are designed and arranged around the rolling body to provide stiffness and damping. Stiffeners (7,8) are used to enhance the behavior of the metallic yield dampers. The concept and the operation principles are stated in a patent [28].

From its name, the roll-n-cage isolation bearing adopts the rolling mechanism to cut off the load path between the isolated object and its base. Such rolling mechanism offers minimal degree of object-base coupling as it requires lower

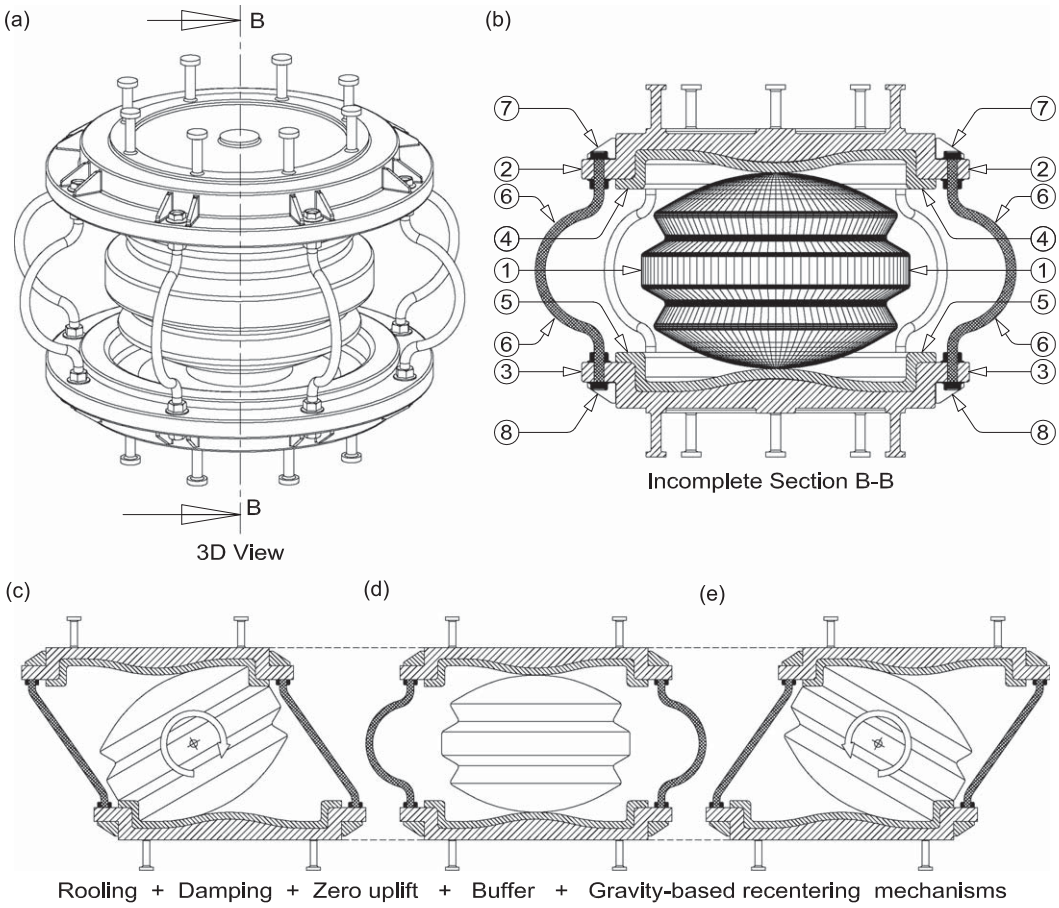

Fig. 1. (a) 3D view of the proposed RNC isolator, (b) partial sectional elevation of the RNC isolator, (c) extremely deformed position to the left of the RNC isolator, (d) neutral position of the RNC isolator, and (e) extremely deformed position to the right of the RNC isolator.

force to roll if compared to sliding mechanism. As a consequence, rolling approaches more the ideal isolation concept which requires a total horizontal separation. However, a system with minimum resistance to lateral motion is susceptible to shaking under minor vibrations and may end up in a different location after an earthquake and continue to dislocate under aftershocks. To avoid these side effects in the RNC isolator, it is provided with a number of metallic yield dampers (6) as a cage to provide suitable stiffness under minor vibrations and damping to limit the vibrational displacement amplitude. They are shaped and arranged as shown in Fig. 1 to provide enough extension during deformation and to exhibit the same shear strain in any horizontal direction.

The RNC has a built-in buffer mechanism to limit the displacement to a predetermined value under severe earthquakes as illustrated in Fig. 1(c,e). During the maximum displacement position, the less stiff plates (4) and (5) act as shock absorbers as shown in Fig. 1(c,e) to reduce the possible shock of the rolling body (1) with the vertical side walls of the bearing plates (2,3) during extreme earthquakes.

After being dislocated, the isolated object must return back to its original position before excitation. So, the RNC isolator is provided with an efficient gravity-based recentering mechanism through the elliptically shaped rolling body (1), shown in Fig. 1(b), along with the weight of the supported object. Such mechanism works as follows: (i) At neutral position, where there is no excitation as shown in Fig. 2(a,b), the isolated object weight has the same line of action of its reaction. Therefore, the developed restoring moment M_r is zero, keeping steady situation. (ii) As the relative motion between the isolated object and the ground initiates, an eccentricity or offset appears between the two vertical lines of action of the weight and its upward reaction as shown in Fig. 2(c,d). This eccentricity is equal to the relative displacement between the isolated object and the ground. Therefore, a restoring couple M_r is generated opposite to the motion-causing couple as illustrated in Fig. 2(c) to re-center the isolated object as in Fig. 2(a,b).

The RNC isolator geometry is designed to prevent vertical displacements of the superstructure during the excitation duration, as shown in Fig. 1(c–e), what prevents vertical accelerations. This is achieved by means of the properly designed curvatures of the inner faces of the stiff upper and lower plates (2,3) and the constant thickness of the less stiff neoprene plates (4,5) shown in Fig. 1(b). Such geometry absorbs exactly the vertical elevation of the isolated superstructure due to rolling of the elliptical body (1) keeping the same vertical offset between the upper and lower plates (2,3) as illustrated in Fig. 1(c–e) by dashed horizontal lines. This guarantees that the RNC isolator does not modify the vertical component of the acceleration as recommended by international codes.

A stiff rolling body sandwiched between two horizontal stiff plates has a point contact with each of them, which is not sufficient to support higher vertical loads. In the RNC isolator, the bearing area is increased by inserting the less stiff plates (4,5) between the rolling body (1) and the upper and lower stiff plates (2,3), respectively.

In brief, the main feature of the RNC isolation system is that it allows great decoupling between an isolated object and its base during earthquake while keeping enough resistance to significant vibrations under minor excitations, exhibiting damping and no uplift. Then, returns back to its neutral position before excitation without exceeding a predetermined maximum translation limit.

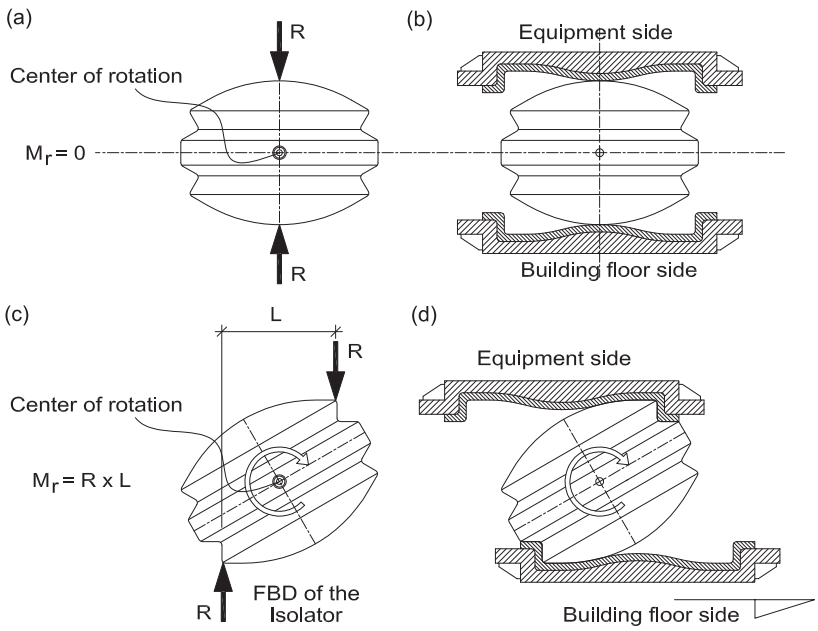

Fig. 2. Gravity-based recentering mechanism: (a,b) neutral position, and (c,d) deformed position.

3. Mechanical characteristics

The general-purpose finite element code ANSYS *Multiphysics* [29] has been used to enable computer-aided design and testing of the RNC isolation system. For a desired configuration of the RNC system, the following steps are followed:

- Design and modeling of the individual components of the RNC isolation system: rolling body (1), upper and lower stiff bearing plates (2,3) and less stiff plates (4,5), metallic yield dampers (6) and bearing plates stiffeners (7,8).
- Assembly of the individual components to set up the whole isolator and identification of all contact conditions among them.
- Definition and assignment of materials for each individual component.
- Selection of appropriate finite element type and mesh size according to the expected behavior of the component materials.
- Assignment of boundary conditions through nodal constraints and nodal restraints.
- Static application of the vertical equipment weight and running full nonlinear analysis to capture all nonlinearities arising from the load application.
- Dynamic application of the horizontal ground motion starting from the last load step in the previous static analysis and running of full nonlinear transient dynamic analysis.
- Analysis of the results.

Through this scheme, a real scale model is designed. An extensive and detailed series of tests is carried out in a machine-like environment, which accurately simulates the response of the device subjected to a testing machine. This allows fully identification of the RNC mechanical characteristics before its construction. In machine-like testing, the topmost surface of the modeled RNC unit is allowed to move vertically (without rotation) under the equipment own weight but it is always kept fixed in horizontal direction. The lowermost surface of the RNC unit is kept always fixed in the vertical direction. In horizontal direction, it is kept fixed only during the vertical application of the equipment own weight. When the ground motion is applied, the lowermost surface is released horizontally without rotation. The neoprene plates (4,5) are completely glued to the inner surfaces of the upper and lower steel bearing plates (2,3), while they are kept in rolling contact with the rolling body (1).

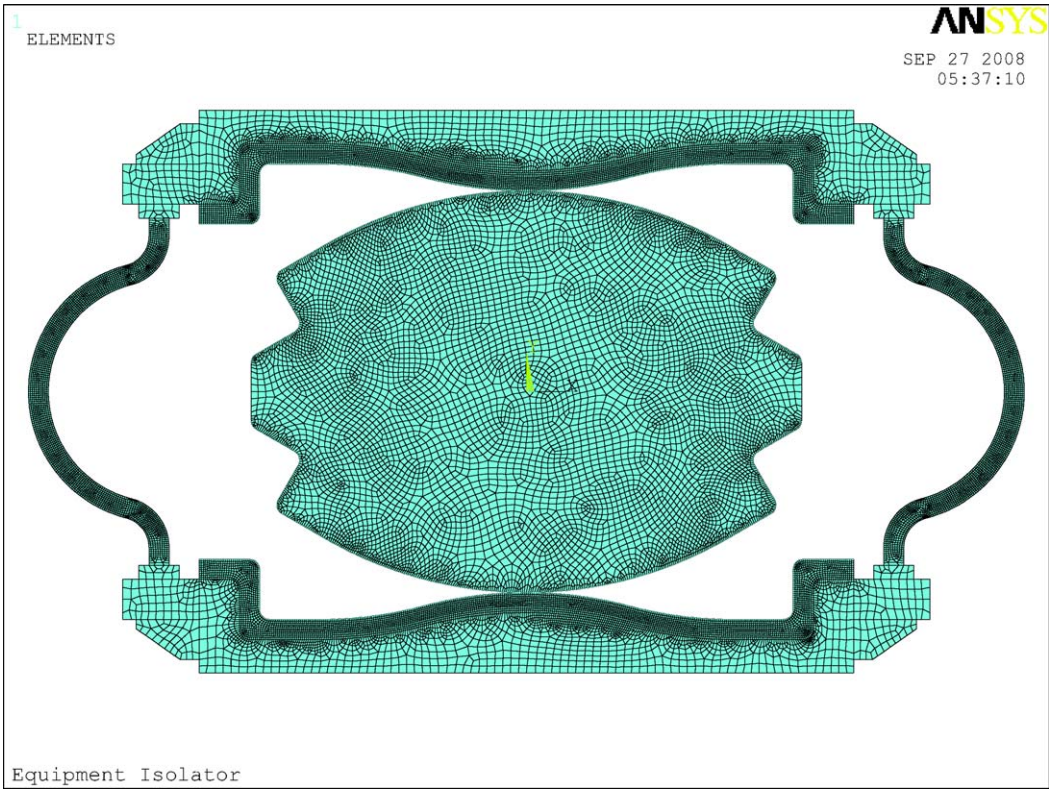

Fig. 3. Finite element model by ANSYS, non-deformed shape.

The RNC unit exhibits three main types of nonlinearities:

1. Contact, which is highly nonlinear and status-dependent.
2. Geometric nonlinearity due to large strains, which lead to changing the geometry of some components as they deflects.
3. Material nonlinearity due to hyperelastic and plastic behaviors of neoprene and mild steel, respectively.

An example of the RNC isolator shown in Fig. 1 is designed for this study. The rolling body (1), top stiff plate (2), and lower stiff plate (3) are made of steel. The metallic yield dampers (6) are made of mild steel. The less stiff plates (4,5) are made of neoprene. The distances between the furthermost points are 0.496 m horizontally and 0.28 m vertically.

To determine the maximum vertical load capacity of the proposed RNC isolator, a trial and error procedure has been carried out using ANSYS such that the vertical strain in the neoprene plates (4,5) does not exceed 30 percent as

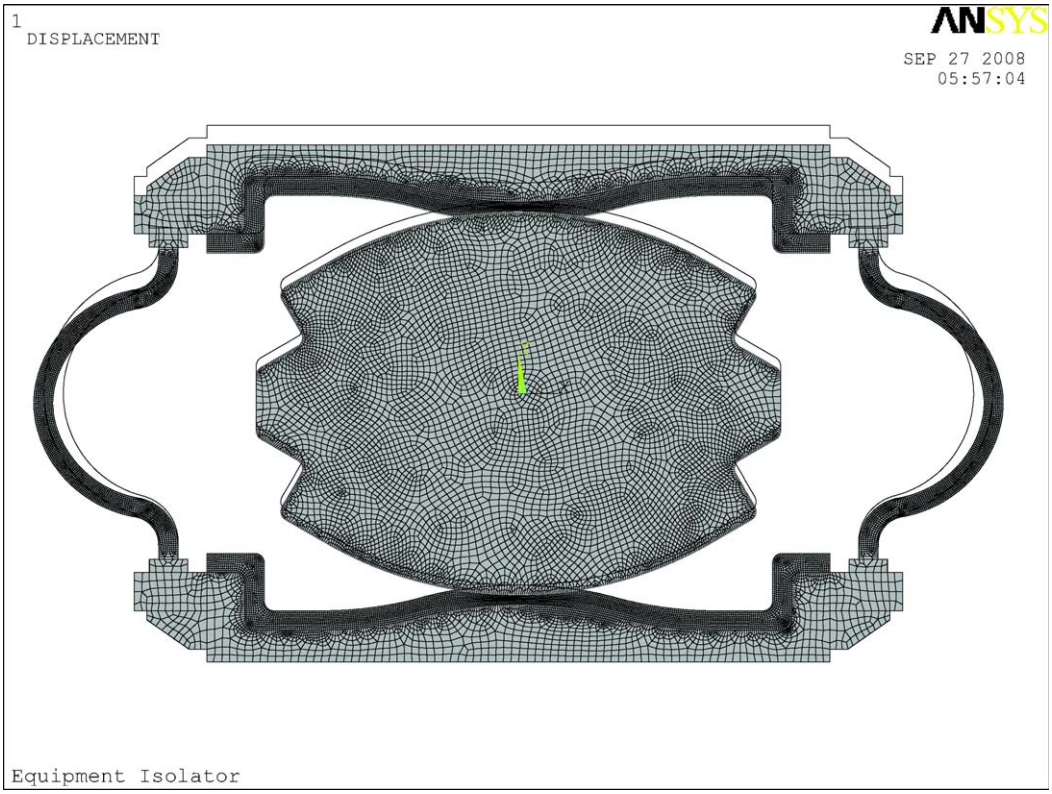

Fig. 4. Finite element model by ANSYS, non-deformed + deformed shape due to equipment weight.

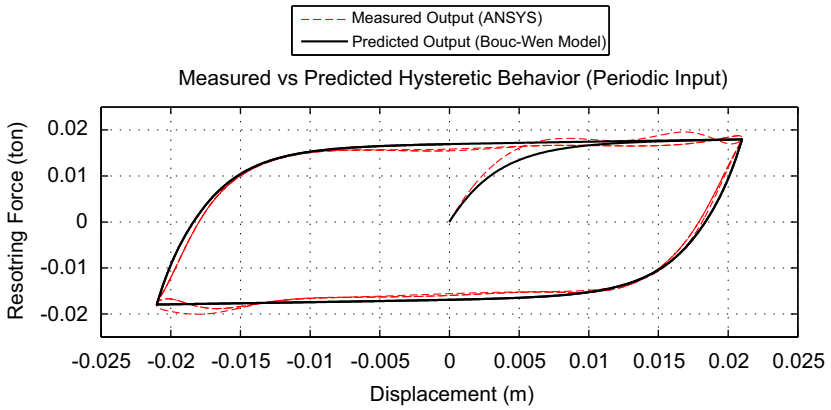

Fig. 5. Measured vs. calculated restoring force for 20% shear strain.

recommended by [30]. As a result, the designed RNC isolator is able to support a maximum weight of 60 kN. Figs. 3 and 4, respectively, show the overall behavior of the assembled RNC unit before and after the static application of the vertical own weight of the supported equipment. The meshing is much more dense in components that exhibit nonlinear behavior (neoprene plates, metallic yield dampers and rolling contact surfaces) if compared to other components that behave linearly (steel bearing plates and rolling body). Also, the behavior of the neoprene plates under loads seems to be realistic. Indeed, Fig. 4 shows how these neoprene plates get deformed and how the corresponding contact areas with the rolling body increase, which translates into higher capacity to support vertical loads. Moreover, the RNC unit shows no lateral motion during this loading stage, in which the topmost surface exhibits the maximum vertical displacement (without rotation) contrary to the lowermost surface which is fixed vertically and exhibits no rotation.

Starting from the last load step of the performed static analysis, a periodic horizontal displacement is applied at the lowermost surface of the RNC isolator, and the resulting force at the topmost surface is calculated. This force–displacement relationship is displayed in Fig. 5 in dashed line. From this figure, the following mechanical characteristics are obtained: (1) pre-yield stiffness of 30 kN/m; (2) post-yield stiffness of 0.229 kN/m; (3) yield displacement of 2.70 mm; and (4) yield force of 0.084 kN.

4. Modeling and identification

The objective of this section is to obtain an input–output mathematical model to describe in a manageable form the force–displacement relationship exhibited by the RNC isolator. This kind of models are used to represent the restoring force of different classes of isolation systems. In particular, the Bouc–Wen model [31–34] has been extensively used to describe nonlinear hysteretic behaviors. The characterization described in Section 3 has shown that the RNC isolator exhibits a hysteretic behavior (as shown in Fig. 5) that is potentially described by the Bouc–Wen model. Recently, a normalized form of the Bouc–Wen model has been proposed [32,33], where the relation between the force $F_b(t)$ and the displacement $x(t)$ is expressed as

$$F_b(t) = \kappa_x x(t) + \kappa_w w(t), \tag{1}$$

$$\dot{w}(t) = \rho(\dot{x} - \sigma|\dot{x}||w|^{n-1}w - (\sigma - 1)\dot{x}|w|^n), \tag{2}$$

where κ_x, κ_w, ρ, σ and n are parameters, and $w(t)$ is an auxiliary variable.

The normalized Bouc–Wen form provides an exact and explicit expression for the hysteretic limit cycle [32,35]. Moreover, by using a periodic input signal $x(t)$ along with the analytic description of the limit cycle, a robust parametric nonlinear, nonrecursive identification method was presented in [33,34]. This method is used in this paper. For identification, the ANSYS code characterization described in Section 3 is used as the "true" isolator device. A periodic input

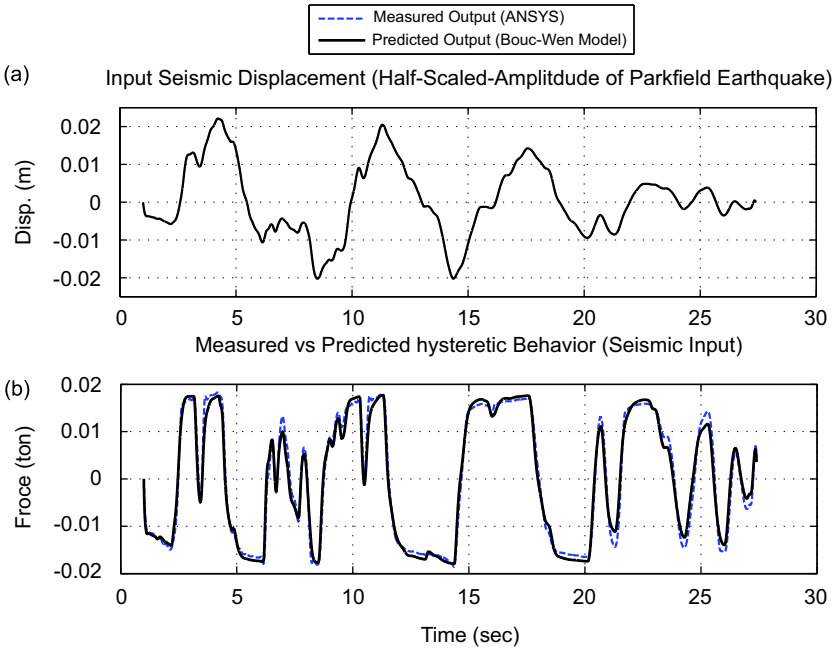

Fig. 6. (a) Half-scaled-amplitude of Parkfield earthquake that is used as input seismic displacement, (b) measured vs. calculated restoring force for seismic input (Parkfield), the relative errors are $\varepsilon_1 = 4.4\%$ and $\varepsilon_\infty = 3.7\%$.

horizontal displacement $x(t)$ is applied at the lowermost surface and the "measured" force is obtained at the topmost surface of the RNC isolator.

The values of the identified parameters of the normalized Bouc–Wen are

$$\kappa_x = 470\,\mathrm{N/m}, \quad \kappa_w = 155\,\mathrm{N}, \quad \rho = 307.68\,\mathrm{m}^{-1}, \quad \sigma = 0.95, \quad n = 1.12.$$

These values guarantee that the model is consistent with basic physical properties as bounded-input bounded-output stability and energy dissipation [35].

In Fig. 5, the measured output restoring force of the isolator is plotted against the calculated one via the identified normalized Bouc–Wen model. The good matching supports the accuracy of the Bouc–Wen model to capture the nonlinear hysteretic behavior of the RNC isolator.

To check the validity of the identified parameters, an actual random seismic displacement (half-scaled-amplitude Parkfield Earthquake) is used as an input for the Bouc–Wen model and the true system. The discrepancy between the measured and predicted outputs, F_m and F_b, is quantified using the L_1 and L_∞-norms and the corresponding relative errors ε:

$$\|f\|_1 = \int_0^{T_e} |f(t)|\,\mathrm{d}t, \quad \|f\|_\infty = \max_{t\in[0,T_e]} |f(t)|, \quad \varepsilon_{1,\infty} = \frac{\|F_m - F_b\|_{1,\infty}}{\|F_m\|_{1,\infty}}. \tag{3}$$

The relative error ε_1 quantifies the ratio of the bounded area between the output curves to the area of the measured force along the excitation duration T_e, while ε_∞ measures the relative deviation of the peak force.

Fig. 6 shows the close matching of both measured and predicted output curves with a relatively small error. Hence, the Bouc–Wen model can be considered a good practical mathematical description of the proposed RNC isolator for further analysis.

5. Implementation

In this section, we consider the case of equipments mounted on a raised floor. The raised floor is connected to the 7th floor of a primary eight storey structure (Fig. 7) through RNC isolators to examine their ability to mitigate the response of equipment housed in upper floors where the seismic acceleration is significantly amplified and the motion contains strong components at long periods. In this implementation, four RNC isolators are used with the configuration shown in Fig. 1 and the mechanical characteristics defined in Section 2.

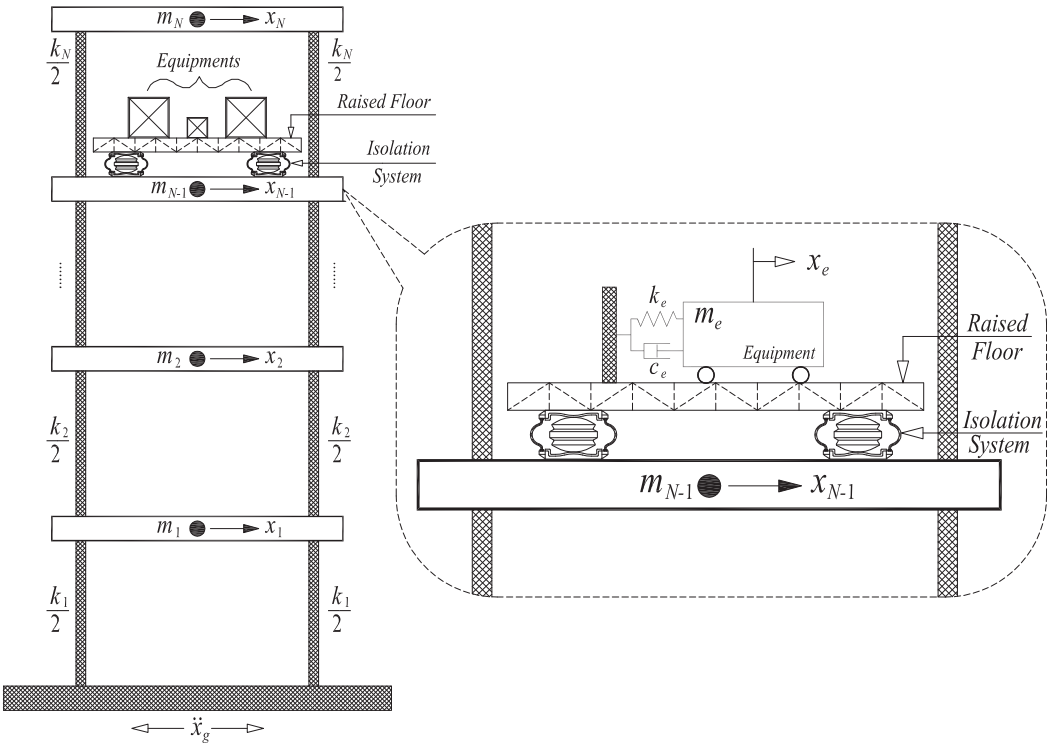

Fig. 7. Idealized building, raised-floor and equipment model.

For comparison purposes, three cases are studied as illustrated in Fig. 8: (a) the isolated raised floor is installed in a fixed base structure, *case* I; (b) non-isolated equipment is housed in a structure isolated by RNC isolators scaled to support the whole housing structure, *case* II; (c) non-isolated equipment is housed in a fixed-base structure, *case* III. In all cases, the structure has the same characteristics.

The supporting structure is a reinforced concrete moment resisting frame modeled as a shear building, where all significant vibrational modes, the structure–equipment interaction, and the isolator nonlinearities are included in the performed analysis in order to get more realistic results. Three example structures are considered having lateral stiffness matrices $\frac{1}{2}\mathbf{K}_s$, $\mathbf{K}_s$ and $2\mathbf{K}_s$. The structural damping ratio for all modes is fixed to 2 percent of the critical damping. The raised floor is assumed to be extremely rigid in horizontal direction. The equipment is modeled as a SDOF system connected to the raised floor through a linear damper with damping coefficient c_e and a linear spring with lateral stiffness k_e as shown in Fig. 7. This stiffness can be modified to tune the equipment to different frequencies. The equipment damping is assumed to be equal to the structural damping. The natural frequencies and effective modal masses of the fixed-base structures and the structure isolated by a suitably scaled RNC isolator (without equipment) are shown in Table 1.

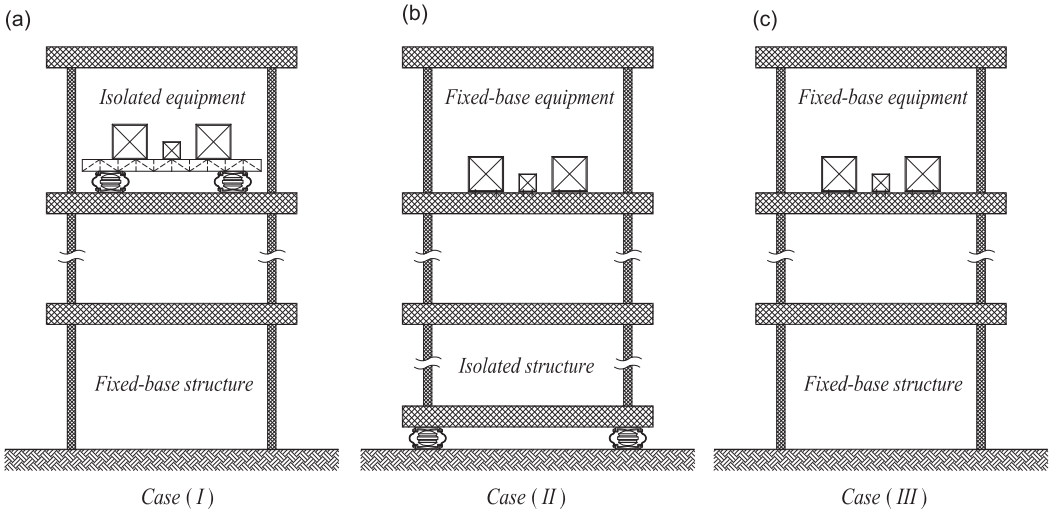

Fig. 8. (a) The case of isolated raised-floor housed in a fixed-base structure, (b) the case of fixed-base equipment housed in an isolated-base structure, (c) the case of fixed-base equipment housed in a fixed-base structure.

Table 1
Modal properties of example structures without equipment.

	Mode number							
	Isolator	1	2	3	4	5	6	7	8
Fixed-base structure, stiffness $= \frac{1}{2}K_s$									
Frequency (Hz)		2.860	8.472	13.762	18.535	22.614	25.860	28.184	29.557
Period (s)		0.350	0.118	0.073	0.054	0.044	0.039	0.035	0.034
Modal participation mass ratios		0.858	0.091	0.029	0.013	0.006	0.003	0.000	0.000
Fixed-base structure, stiffness $= K_s$									
Frequency (Hz)		3.857	11.425	18.560	24.996	30.497	34.875	38.009	39.861
Period (s)		0.259	0.088	0.054	0.040	0.033	0.029	0.026	0.025
Modal participation mass ratios		0.858	0.091	0.029	0.013	0.006	0.003	0.000	0.000
Fixed-base structure, stiffness $= 2K_s$									
Frequency (Hz)		5.104	15.118	24.56	33.076	40.355	46.148	50.295	52.745
Period (s)		0.196	0.066	0.041	0.030	0.025	0.022	0.020	0.019
Modal participation mass ratios		0.858	0.091	0.029	0.013	0.006	0.003	0.000	0.000
Base-isolated structure, stiffness $= K_s$									
Frequency (Hz)	0.220	7.007	13.837	20.301	26.171	31.223	35.266	38.174	39.900
Period (s)	4.552	0.143	0.072	0.049	0.038	0.032	0.028	0.026	0.025
Modal participation mass ratios	0.999	0.001	0.000	0.000	0.000	0.000	0.000	0.000	0.000

To achieve effective isolation, it is necessary to increase the period of the isolated equipment to large values, which typically are larger than those required for effective isolation of buildings [5]. Accordingly, the equipment has a fundamental period of 0.0065 s (in the case of relatively rigid equipment) and 8.546 s in non-isolated and isolated conditions, respectively. The considered mass range of the equipment is 1–3 percent of the total mass of the structure (including the base mass).

Isolators are normally designed to allow a travel distance greater than that which would occur during design earthquakes. In this paper, the maximum rolling displacements of the RNC isolators during earthquakes were determined without using the built-in buffer (stoppers) mechanism, to check whether they are affordable or not. Then, the buffer is designed to allow for rolling displacements a little bit higher. During stronger earthquakes, the rolling displacements may be exceeded but the buffer prevents such excessive displacements with minimal shock. This last point has not been studied in this paper because there is no available model, at the moment, for the built-in buffer mechanism of the RNC isolator.

5.1. Equations of motion

The following assumptions are made for the structural system under consideration: (1) the superstructure remains within the elastic limit during the earthquake excitation and the nonlinearity is concentrated only at the isolation elements; (2) the floors are assumed rigid in its own plane and the mass is lumped at each floor level; (3) the columns are inextensible and weightless providing the lateral stiffness; (4) the system is subjected to a single horizontal component of the earthquake ground motion; (5) the effects of soil–structure interaction are not taken into consideration.

The equations of motion for the fixed-base structure under earthquake ground acceleration are expressed in matrix form as

$$\mathbf{M}_s\ddot{\mathbf{x}}_s + \mathbf{C}_s\dot{\mathbf{x}}_s + \mathbf{K}_s\mathbf{x}_s = -\mathbf{M}_s\mathbf{r}\ddot{x}_g, \tag{4}$$

where $\mathbf{M}_s$, $\mathbf{C}_s$ and $\mathbf{K}_s$ are the mass, damping and stiffness matrices of the superstructure, respectively; $\mathbf{x}_s = \{x_1, x_2, ..., x_N\}^{\mathrm{T}}$, $\dot{\mathbf{x}}_s$ and $\ddot{\mathbf{x}}_s$ are the relative floor displacement, velocity and acceleration vectors, respectively; $\ddot{x}_g$ is the earthquake ground acceleration; and $\mathbf{r}$ is the vector of influence coefficients. In the case of the isolated structure, the right-hand-side in Eq. (4) is replaced by $-\mathbf{M}_s\mathbf{r}(\ddot{x}_b + \ddot{x}_g)$, where $\ddot{x}_b$ is the relative acceleration of the base mass.

The corresponding equations of motion for the equipment and the isolated raised floor mounted to a building floor under earthquake ground acceleration is expressed by

$$m_e\ddot{x}_e + c_e\dot{x}_e + k_e x_e = -m_e(\ddot{x}_f + \ddot{x}_r), \tag{5}$$

$$m_r\ddot{x}_r - c_e\dot{x}_e - k_e x_e + \eta F_b = -m_r\ddot{x}_f, \tag{6}$$

where the subscript r denotes raised floor; e refers to equipment; f denotes mounting floor and $\ddot{x}_f = \ddot{x}_7 + \ddot{x}_g$, where the 7th floor is the housing floor of the equipment. The restoring force developed in the isolation system of the raised floor F_b is modeled using the normalized Bouc–Wen hysteretic model in Eqs. (1) and (2).

In the case of the isolated structure, see Fig. 8(b), the corresponding equation of motion for the base mass under earthquake ground acceleration is expressed by

$$m_b\ddot{x}_b - c_1\dot{x}_1 - k_1 x_1 + \eta F_b = -m_b\ddot{x}_g, \tag{7}$$

where m_b and F_b are the base mass and the restoring force developed in the isolation system of the entire building, respectively; c_1 and k_1 are the first story damping and stiffness, respectively; and η is the number of isolators.

5.2. Energy balance

The proposed RNC isolator reduces the dynamic response of the isolated object by filtering the seismic excitations and by dissipating energy through metallic yield dampers, thereby reducing the input energy and seismic demand. Energy quantities provide a very useful measure for assessing the isolator performance since they involve all the response variables (displacements, velocity and accelerations of all degrees of freedom) and therefore represent overall response of the structure. As the energy quantities are scalar, only a single equation for the entire structure can be derived irrespective of the number of degrees of freedom in the structure.

The total absolute energy E_i of a base isolated structure at each time instant can be decomposed in the form [36]

$$E_i = E_k + E_p + E_s + E_\xi + E_y, \tag{8}$$

where E_k, E_p and E_s are kinetic energy, potential energy due to vertical displacement (always zero in this study because the proposed RNC isolator is designed to prevent vertical uplift) of the isolated object during rolling, and strain energy, respectively. These components represent the conservative energy in the system. E_ξ and E_y are the non-conservative energies due to structural damping and yielding of metallic dampers, respectively.

5.3. Simulation tool

The structural and equipment responses have been obtained by means of the Structural Analysis Program SAP2000 *advanced* [37]. The dynamic response is calculated using the fast nonlinear analysis FNA [38] which is particularly suitable for structures having limited number of points or members in which nonlinear behavior takes place when subjected to static or dynamic loading. This FNA makes the nonlinear analysis almost as fast as a linear analysis keeping the accuracy of accurate direct integration methods. The FNA method is applied to both the static and dynamic analysis of linear or nonlinear structural systems. A limited number of predefined nonlinear elements are assumed to exist. Stiffness and mass orthogonal load dependent Ritz vectors of the elastic structural system are used to reduce the size of the nonlinear system to be solved. The forces in the nonlinear elements are calculated by iteration at the end of each time or load step. The uncoupled modal equations are solved exactly for each time increment.

The RNC isolator is modeled as a nonlinear support in SAP2000. The dynamic behavior of the RNC isolator is governed by the hysteretic Bouc–Wen model [31], while the rest of the structure is assumed to behave linearly. The parameters of the Bouc–Wen model have been identified in Section 4 and incorporated into the simulation code [37]. The masses of the isolator's components are included in the nonlinear dynamic analysis.

5.4. Displacement demand against isolator height

Practically, isolation of inner equipment necessitates isolators of relatively low profiles due to the limited storey heights. The RNC isolator offers adequate bearing capacity to support equipment. Therefore, its dimensions are mainly designed

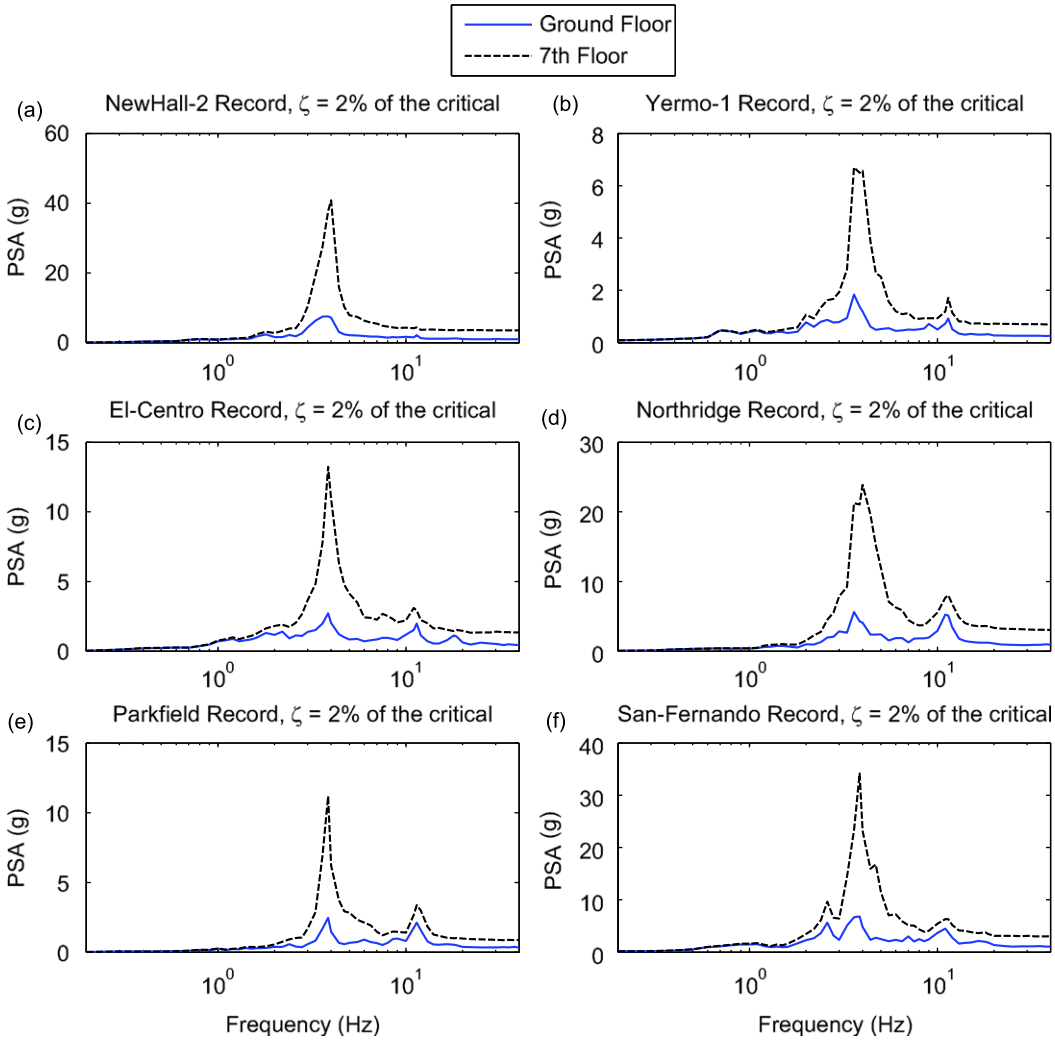

Fig. 9. Response spectra for the ground and the 7th floor accelerations under the following earthquakes: (a) New-Hall 90°, (b) Yermo 0°, (c) El-Centro, (d) Northridge, (e) Parkfield, and (f) San-Fernando. The structural damping ratio is 2% of the critical.

according to the displacement demand. One of the main parameters that control the RNC isolator rolling displacement is its height. A set of RNC isolators having the same mechanical characteristics, given in Section 3, but of different heights have been used in this study according to the displacement demand. The aim is to fulfill the displacement demand under various excitations but with the lowest possible isolator profile. Four displacement demands of 0.11, 0.22, 0.33, 0.41 m have been considered and the corresponding total heights of the RNC isolators have been determined, being 0.28, 0.56, 0.76, 0.89 m, respectively. Other RNC isolators that provide higher displacement demands have been also used in this study, but they are not mentioned in this paper because their dimensions might be seen impractical for isolation of housed equipments.

6. Numerical assessment

Fig. 9 shows the response spectra of the ground accelerations and the 7th floor accelerations, at 2 percent structural damping ratio, when the fixed-base structure under study (cases I and III in Fig. 8(a,c)) is subjected to six selected earthquakes. Fig. 9 illustrates the amplification of the acceleration response in upper floors. Consequently, an equipment mounted on upper floors will be subjected to much stronger excitations than if it is mounted on lower floors.

In this scenario, the purpose of this section is to analyze the efficiency of the RNC isolation device in reducing the acceleration of the equipment while keeping affordable displacements. This analysis is performed in two complementary directions: (1) an example structure is subjected to a series of actual earthquakes; (2) the three example structures are subjected to constant-amplitude variable-frequency harmonic ground motions.

6.1. Actual earthquakes

The structure considered in this section has a lateral stiffness $\mathbf{K}_s$, and the three cases shown in Fig. 8 are analyzed. The dynamic properties of the structure for isolated and fixed-base conditions are given in Table 1. The equipment mass is taken as 3 percent of the total structural mass.

Fig. 10 displays the absolute acceleration time history of the equipment for the three cases under study (illustrated in Fig. 8) subjected to El-Centro earthquake. Fig. 11 displays the corresponding time history of the equipment displacement

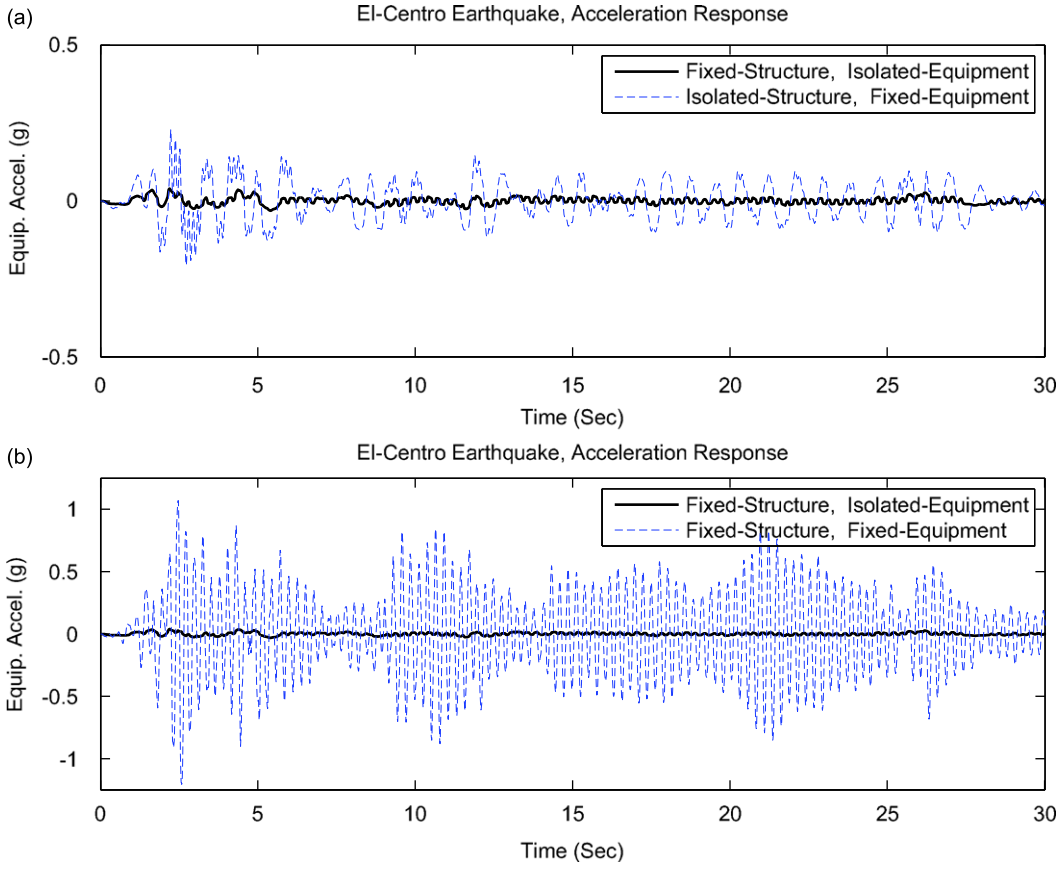

Fig. 10. Absolute acceleration response time history of equipment under El-Centro earthquake: (a) isolated-raised floor housed in a fixed-base structure vs. fixed-base equipment housed in an isolated-base structure (*case* I vs. *case* II), and (b) isolated-raised floor housed in a fixed-base structure vs. fixed-base equipment housed in a fixed-base structure (*case* I vs. *case* III).

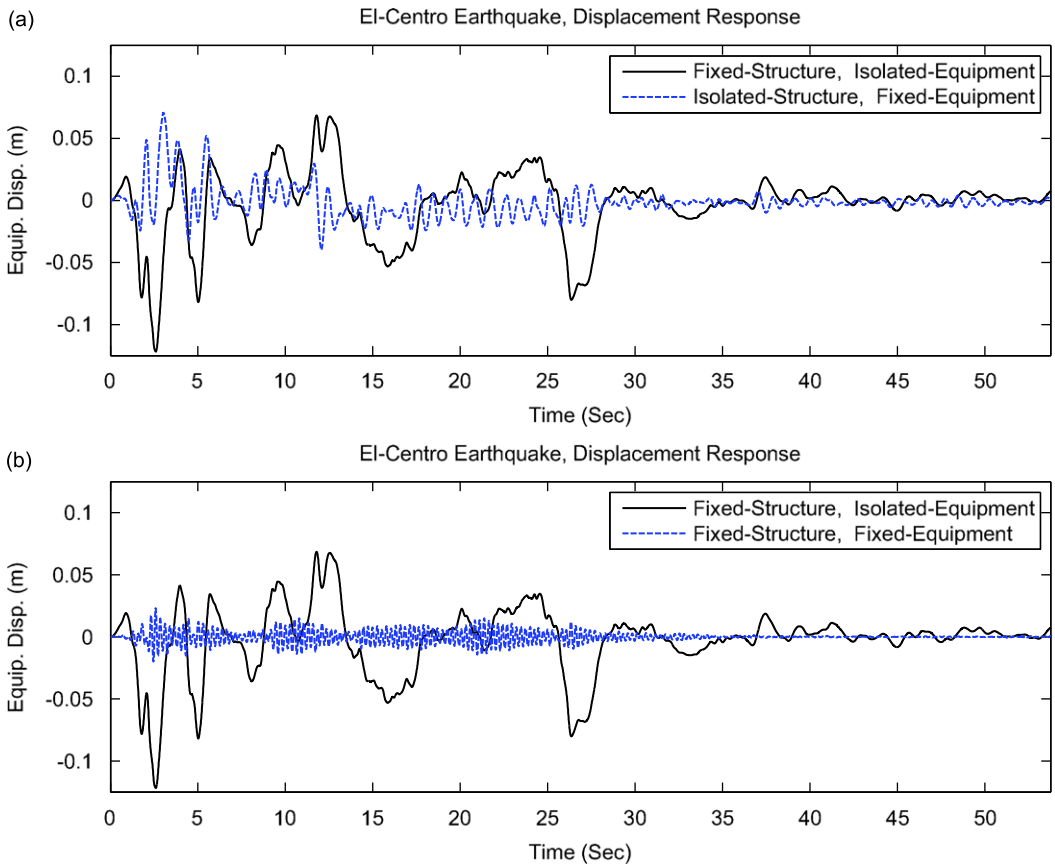

Fig. 11. Time history of the equipment displacement relative to the mounting building floor under El-Centro earthquake: (a) isolated-raised floor housed in a fixed-base structure vs. fixed-base equipment housed in an isolated-base structure (*case* I vs. *case* II), and (b) isolated-raised floor housed in a fixed-base structure vs. fixed-base equipment housed in a fixed-base structure (*case* I vs. *case* III).

relative to the mounting building floor. It can be observed that the acceleration of the equipment is greatly reduced when comparing case I (fixed structure with RNC-isolated raised floor) to case III (fixed structure with fixed equipment) in Fig. 10(b). This reduction is also significant when case I is compared to case II (isolated structure, using RNC isolator, with fixed equipment) in Fig. 10(a). Although cases I and II represent two approaches for equipment isolation, it is evident from Fig. 10(a) that the first approach is superior to the second one. Further, the former approach (case I) is expected to be more economic than the later one (case II). Fig. 11 shows that the associated displacement of the equipment in isolated cases I and II are larger than the displacement in the fixed case III, but they remain affordable. This emphasizes the ability of the proposed RNC isolator to greatly attenuate the equipment acceleration while keeping reasonable rolling displacement.

In Fig. 12, the effect of long-period ground excitations is considered using the Mexico-city earthquake. By comparing the dashed lines in both top and bottom plots in Fig. 12, it is observed that the acceleration response of case II is close to that of case III, i.e. isolation of the whole housing structure may not be the right decision to protect equipment under such excitation. On the other hand, the first approach (case I, represented by solid line in Fig. 12) reduces significantly the equipment acceleration response under the same long-period excitation.

The energy result gives additional information, which cannot be obtained from the response time history [19]. Fig. 13 shows the time history of the recoverable energy of the equipment (kinetic energy + strain energy) under Northridge and San Fernando earthquakes for cases I and III. It is observed that the maximum recoverable energy is considerably reduced in the isolated case. This highlights the ability of the proposed RNC isolator to offer a great horizontal flexibility that shifts the fundamental period of the isolated system to a high value (8.546 s in this study), which falls in a frequency range in which many of the recorded earthquakes have considerable energy.

Fig. 14 shows the peak absolute acceleration and relative displacement of the isolated (case I) and non-isolated (case III) equipment for eight selected earthquakes. Fig. 14(a) shows the general effectiveness of the proposed isolator in reducing a major part of the equipment acceleration. It is clear that the proposed system is capable of eliminating up to 98 percent of the equipment acceleration as for the Northridge earthquake, record number 6. This significant reduction is mainly due to the minimal base shear forces transmitted to the raised floor through the RNC isolator. This is due to the great decoupling offered by: (i) the rolling concept upon which the RNC isolator is based on; (ii) the low post-yield stiffness of the designed

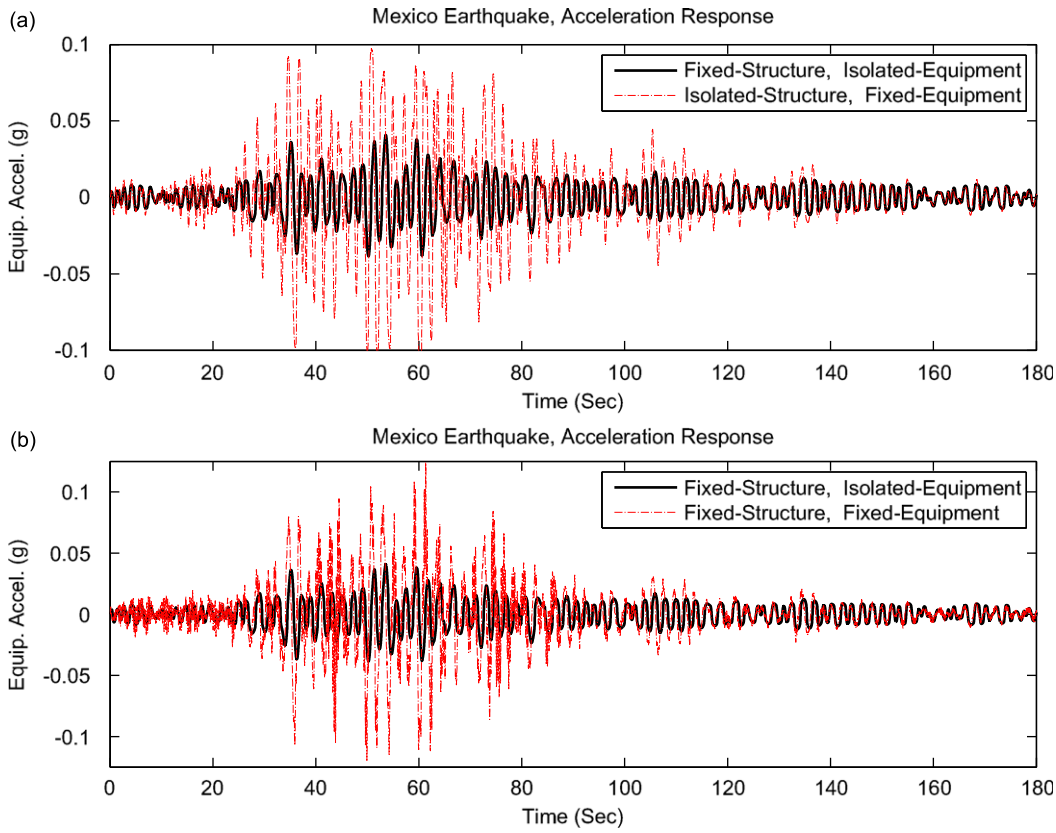

Fig. 12. Absolute acceleration response time history of equipment under Mexico-city earthquake: (a) isolated-raised floor housed in a fixed-base structure vs. fixed-base equipment housed in an isolated-base structure (*case* I vs. *case* II), and (b) isolated-raised floor housed in a fixed-base structure vs. fixed-base equipment housed in a fixed-base structure (*case* I vs. *case* III).

RNC isolator, as characterized in Section 3. This decrease in acceleration is accompanied with some lateral displacement due to rolling. As shown in Fig. 14(b) these rolling displacements are in a reasonable range and seem to be small if compared to the overall structural dimensions. Indeed, the maximum rolling displacement of the isolated equipment corresponds to (record number 8) San Fernando earthquake (0.373 m) that contains strong motion at lower frequencies, which are close to that of the isolated equipment. However, the built-in recentering and damping mechanisms prevent permanent dislocation and allow for efficient restoration and motion damping. Moreover, the inherent buffer prevents undesirable excessive displacements in the lateral direction.

Further, the primary structures in cases I and III (Fig. 8) are excited by 36 actual earthquake ground motions to make sure that the good performance observed before can be achieved for a wider range of earthquake excitations. The displacement and acceleration responses of isolated vs. non-isolated equipment are summarized in Table 2. Under a variety of ground motion excitations having different characteristics, the proposed RNC isolator shows significant efficiency in mitigating the equipment acceleration response while exhibiting reasonable rolling displacement. Even under long-period excitations such as the Mexico-city earthquake, the RNC isolator still shows significant efficiency.

Regarding the displacement demand and the isolator height mentioned in Section 5.4, the results of Table 2 provide useful information for that purpose. The displacements of isolated equipment, sixth column from left in Table 2, are grouped with respect to the displacement demands of the four RNC isolators, mentioned in Section 5.4, as shown in Table 3. The third column from left in Table 3 gives the number of earthquakes that demand displacements that can be fulfilled by each isolator. From Table 3, it can be seen that a relatively low profile of 0.56 m can fulfill the displacement demands of up to 75 percent of the cases considered in Table 2, and up to 92 percent of the cases are within the capacity of the 0.76 m height RNC isolator.

6.2. Harmonic excitations

To examine the effect of equipment mass and structural stiffness variations on the isolated equipment response, two equipment/structure mass ratios of 1 percent and 3 percent are used together with the three example structures having

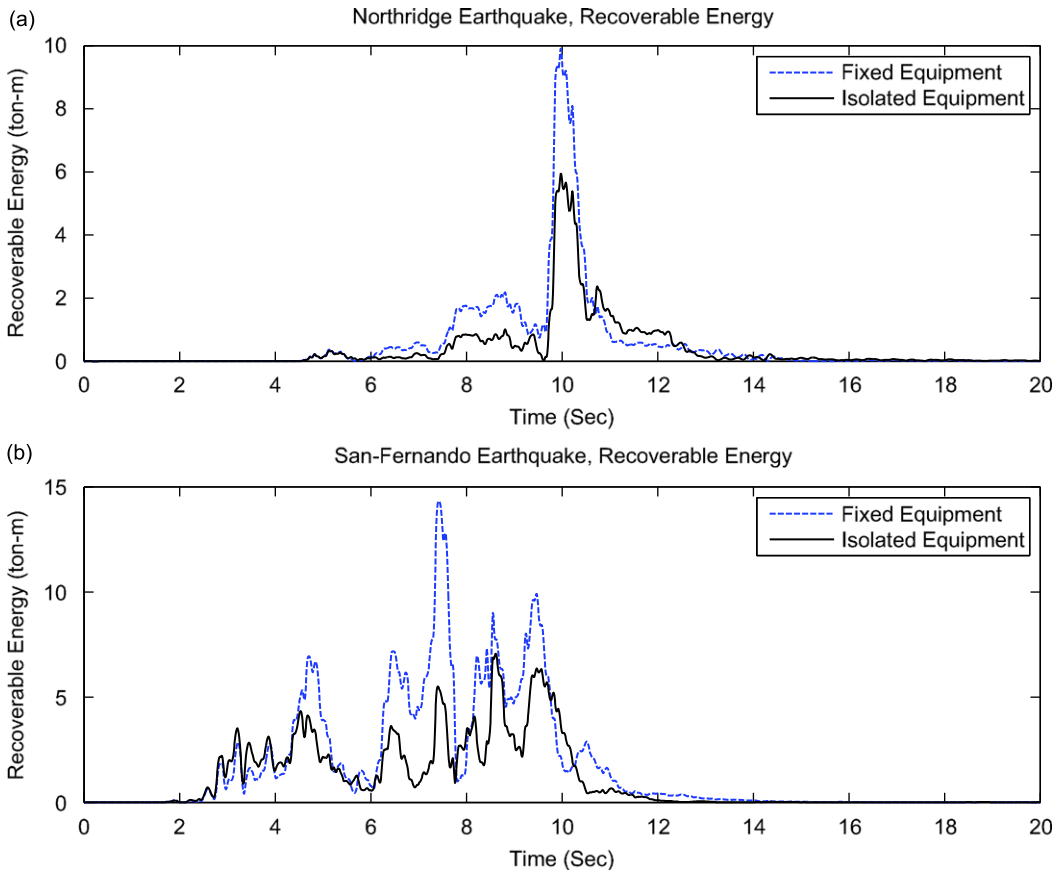

Fig. 13. Recoverable energy time history: (a) Northridge earthquake, and (b) San-Fernando earthquake.

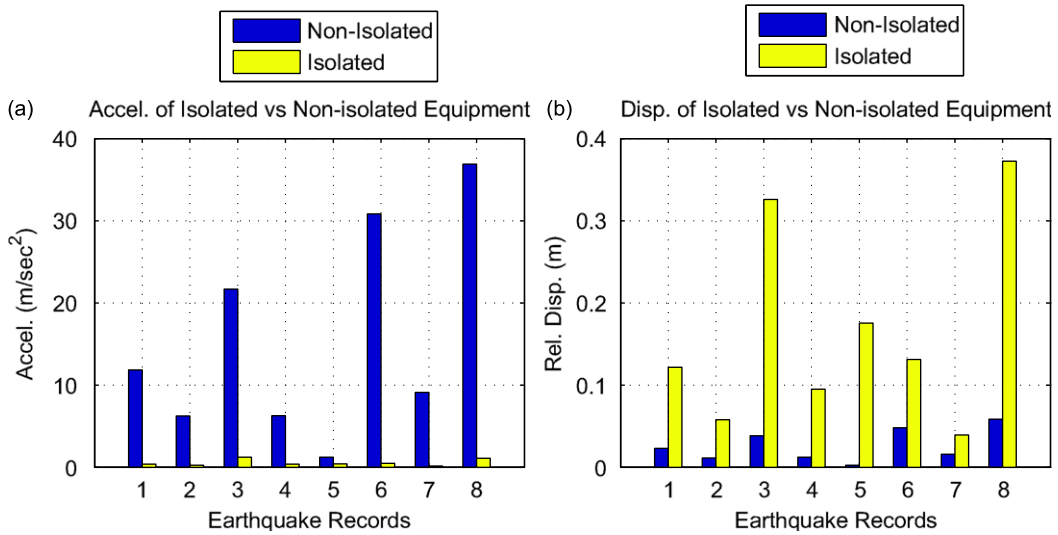

Fig. 14. (a) Acceleration response of isolated vs. non-isolated equipment for eight earthquake records, (b) isolated vs. non-isolated associated relative displacement between the equipment and the housing 7th floor. The eight earthquake records are: (1) El-Centro, (2) Kern, (3) Kobe, (4) Loma-Prieta, (5) Mexico, (6) Northridge, (7) Parkfield, and (8) San-Fernando.

lateral stiffness $\frac{1}{2}\mathbf{K}_s$, $\mathbf{K}_s$ and $2\mathbf{K}_s$, whose dynamic properties are given in Table 1. Only cases I and III in Fig. 8 are considered in this analysis. The primary structures are subjected to different harmonic ground excitations with an amplitude 0.5 g and different frequencies (f_g) ranging from 1.00 to 40 Hz with an increment equal to 0.25 Hz.

Table 2
Response summary under 36 seismic excitations.

Equipment/structure mass ratio = 1% and structure's lateral stiffness = K_s							
No.	Earthquake		Non-isolated equipment		Isolated equipment		Reduction (%)
	Record	Peak accel. (g)	Rel. disp. (m)	Peak accel. (m/s^2)	Rel. disp.	Peak accel. (m/s^2)	
1	ALTADENA 0°	0.448	0.0292	15.8977	0.0420	0.3299	98
2	ALTADENA 90°	0.179	0.0071	4.2643	0.0084	0.1332	97
3	ARRAY06 0°	0.376	0.0202	11.2952	0.3049	0.6873	94
4	ARRAY06 90°	0.437	0.0262	15.0973	0.5764	1.0516	93
5	CORRALIT 0°	0.630	0.0521	28.3104	0.0946	0.5913	98
6	CORRALIT 90°	0.479	0.0255	15.0698	0.1657	0.4749	97
7	HOLLISTE 0°	0.369	0.0144	7.7122	0.1985	0.6898	91
8	HOLLISTE 90°	0.178	0.0168	9.3717	0.1640	0.3360	96
9	LACC-NOR 0°	0.222	0.0106	5.6443	0.0678	0.2995	95
10	LACC-NOR 90°	0.256	0.0246	13.2492	0.0615	0.2506	98
11	LEXINGT 0°	0.442	0.0162	8.7660	0.2068	0.8117	91
12	LEXINGT 90°	0.410	0.0216	11.6343	0.3161	0.9803	92
13	LUCERNE 0°	0.681	0.0081	11.8413	0.1139	0.4093	97
14	LUCERNE 90°	0.703	0.0275	19.9379	0.1089	0.3524	98
15	NEW-HALL 0°	0.590	0.0589	32.7304	0.2893	0.8273	97
16	NEW-HALL 90°	0.583	0.0656	36.1720	0.2005	0.6164	98
17	OAK-WHAF0°	0.287	0.0109	5.7637	0.0896	0.4594	92
18	OAK-WHAF 90°	0.271	0.0131	6.8429	0.1043	0.4266	94
19	PETROLIA 0°	0.590	0.0209	12.3905	0.1315	0.5591	95
20	PETROLIA 90°	0.662	0.0241	13.9574	0.3127	0.9619	93
21	POMONA 0°	0.186	0.0151	9.3387	0.0150	0.1619	98
22	POMONA 90°	0.207	0.0098	6.4272	0.0148	0.1517	98
23	SANTA-MONICA 0°	0.370	0.0180	10.8338	0.0773	0.2874	97
24	SANTA-MONICA 90°	0.883	0.0480	30.8220	0.1311	0.4690	98
25	SYLMAR 0°	0.843	0.0454	25.1010	0.4107	1.2574	95
26	SYLMAR 90°	0.604	0.0206	11.0541	0.2044	0.7543	93
27	YERMO 0°	0.151	0.0143	7.9039	0.1530	0.3247	96
28	YERMO 90°	0.245	0.0137	7.1296	0.2973	0.4596	94
29	EL-CENTRO	0.348	0.0231	11.8343	0.1218	0.3900	97
30	KERN	0.179	0.0112	6.2217	0.0578	0.2296	96
31	KOBE	0.679	0.0384	21.6752	0.3260	1.2067	94
32	LOMA-PRIETA	0.276	0.0121	6.2564	0.0950	0.3893	94
33	MEXICO	0.100	0.0025	1.2171	0.1755	0.4006	67
34	NORTHRIDGE	0.883	0.0480	30.8216	0.1312	0.4691	98
35	PARKFIELD	0.237	0.0157	9.1186	0.0393	0.1510	98
36	SAN-FERNANDO	1.171	0.0584	36.9040	0.3725	1.1073	97

Table 3
Displacement demands and RNC isolator heights.

Isolator height (m)	Equipment rel. disp. (m)	Number of valid cases/total cases	Percentage (%)
0.28	≤ 0.11	14/36	39
0.56	≤ 0.22	27/36	75
0.76	≤ 0.33	33/36	92
0.89	≤ 0.41	35/36	97
The rest	≥ 0.41	1/36	3

Tables 4–6 give the peak values of the absolute acceleration and the relative displacement of the fixed-base and the isolated equipment for each case. By comparing the isolated an fixed-base cases in Tables 4–6, it is found that the proposed RNC isolation system is very effective in reducing the acceleration of the equipment even near the fundamental frequencies of the primary buildings, which are 2.86 Hz for $\frac{1}{2}\mathbf{K}_s$, 3.857 Hz for $\mathbf{K}_s$ and 5.104 Hz for $2\mathbf{K}_s$. In this study, the proposed isolator is designed to provide a great horizontal flexibility, which decreases acceleration significantly. However, this is associated with some lateral displacement on the rolling surface of the isolator. Except for a very low-frequency excitation (where the harmonic excitation frequency is close to that of the isolated equipment), these rolling displacements are within a reasonable range.

By comparing the results for 1 percent and 3 percent equipment/structure mass ratios in Tables 4–6, it is clear that increasing the equipment mass (reducing its frequency) increases the rolling displacement but reduces the equipment

Table 4
The frequency of harmonic base excitations vs. equipment displacement and acceleration responses, at Equipment/Structure mass ratios of 1% and 3%. The structure's lateral stiffness $= \frac{1}{2}K_s$.

Structure's lateral stiffness $= \frac{1}{2}K_s$										
Excitation frequency (Hz)	Equipment/structure mass ratio = 1%				Accel. reduction (%)	Equipment/structure mass ratio = 3%				Accel. reduction (%)
	Fixed-base equipment		Isolated equipment			Fixed-base equipment		Isolated equipment		
	Disp. (m)	Accel. (m/s^2)	Disp. (m)	Accel. (m/s^2)		Disp. (m)	Accel. (m/s^2)	Disp. (m)	Accel. (m/s^2)	
1.00	0.0218	5.7158	0.5972	1.3484	76	0.0227	5.7499	0.7073	1.2181	79
1.25	0.0238	6.3358	0.4653	1.1065	83	0.0248	6.4027	0.5372	1.0044	84
1.50	0.0283	7.6696	0.3709	0.9337	88	0.0298	7.8115	0.4439	0.8525	89
1.75	0.0354	9.8299	0.3105	0.8056	92	0.0370	9.9509	0.3682	0.7399	93
2.00	0.0393	11.0541	0.2707	0.7092	94	0.0423	11.5336	0.3208	0.6543	94
2.25	0.0567	16.3808	0.2342	0.6353	96	0.0634	17.7387	0.2807	0.5872	97
2.50	0.0946	28.0780	0.2109	0.5772	98	0.1141	32.8317	0.2521	0.5335	98
2.75	0.3309	101.4019	0.1899	0.5302	99	0.3409	101.3864	0.2265	0.4895	99
3.00	0.1223	38.7161	0.1709	0.4917	99	0.1040	31.9310	0.2068	0.4527	99
5.00	0.0096	4.5741	0.0899	0.3099	93	0.0094	4.4019	0.1145	0.2690	94
10.00	0.0003	3.6885	0.0382	0.1979	95	0.0004	3.3774	0.0450	0.1599	95
20.00	0.0004	1.5278	0.0119	0.1298	92	0.0004	1.6405	0.0137	0.0941	94
30.00	0.0047	3.2032	0.0058	0.1067	97	0.0042	2.9928	0.0066	0.0721	98
40.00	0.0023	3.6659	0.0037	0.0941	97	0.0023	3.0882	0.0040	0.0605	98

Table 5
The frequency of harmonic base excitations vs. equipment displacement and acceleration responses, at equipment/structure mass ratios of 1% and 3%.

Structure's lateral stiffness $= \frac{1}{2}K_s$										
Excitation frequency (Hz)	Equipment/structure mass ratio = 1%				Accel. reduction (%)	Equipment/structure mass ratio = 3%				Accel. reduction (%)
	Fixed-base equipment		Isolated equipment			Fixed-base equipment		Isolated equipment		
	Disp. (m)	Accel. (m/s^2)	Disp. (m)	Accel. (m/s^2)		Disp. (m)	Accel. (m/s^2)	Disp. (m)	Accel. (m/s^2)	
1.00	0.0112	5.3041	0.5943	1.3425	75	0.0116	5.3198	0.7056	1.2153	77
1.25	0.0117	5.5847	0.4651	1.1002	80	0.0122	5.6133	0.5381	1.0024	82
1.50	0.0130	6.3306	0.3657	0.9374	85	0.0134	6.3807	0.4400	0.8552	87
1.75	0.0151	7.3773	0.3084	0.8163	89	0.0160	7.5719	0.3655	0.7454	90
2.00	0.0146	7.1680	0.2708	0.7224	90	0.0153	7.2847	0.3211	0.6605	91
2.25	0.0170	8.4929	0.2310	0.6478	92	0.0180	8.6994	0.2780	0.5929	93
2.50	0.0188	9.4981	0.2087	0.5878	94	0.0200	9.8071	0.2503	0.5383	95
2.75	0.0274	14.1328	0.1879	0.5390	96	0.0296	14.7626	0.2247	0.4934	97
3.00	0.0337	17.6190	0.1704	0.4987	97	0.0381	19.3891	0.2061	0.4559	98
4.00	0.0779	44.7036	0.1261	0.3901	99	0.0620	34.5002	0.1522	0.3524	99
5.00	0.0143	9.2390	0.0952	0.3209	97	0.0136	8.5542	0.1166	0.2867	97
10.00	0.0031	7.3222	0.0378	0.1993	97	0.0032	7.6626	0.0448	0.1605	98
20.00	0.0004	1.9403	0.0116	0.1304	93	0.0004	1.8249	0.0136	0.0950	95
30.00	0.0021	4.8775	0.0056	0.1072	98	0.0024	4.9283	0.0065	0.0726	99
40.00	0.0030	2.9941	0.0035	0.0944	97	0.0026	2.7371	0.0039	0.0608	98

The structure's lateral stiffness $= K_s$.

acceleration. On the other hand, the variation of the structural stiffness has a minimal influence on the response of the isolated equipment. This is due to the great decoupling of structure–equipment by means of the RNC isolator.

7. Conclusion

In this paper, a novel seismic isolation bearing is proposed as an attempt to approach the ideal isolation concept. It is referred to as roll-n-cage isolator and named after its operation principle. The RNC integrates several passive mechanisms to allow great decoupling between the isolated object and its base during earthquakes, while keeping enough resistance to minor excitations, exhibiting damping and no uplift. Then, it returns back to its neutral position before excitation without

Table 6
The frequency of harmonic base excitations vs. equipment displacement and acceleration responses, at equipment/structure mass ratios of 1% and 3%.

Structure's lateral stiffness $= 2K_s$										
Excitation frequency (Hz)	Equipment/structure mass ratio = 1%				Accel. reduction (%)	Equipment/structure mass ratio = 3%				Accel. reduction (%)
	Fixed-base equipment		Isolated equipment			Fixed-base equipment		Isolated equipment		
	Disp. (m)	Accel. (m/s^2)	Disp. (m)	Accel. (m/s^2)		Disp. (m)	Accel. (m/s^2)	Disp. (m)	Accel. (m/s^2)	
1.00	0.0062	5.1243	0.5932	1.3424	74	0.0064	5.1330	0.7049	1.2156	76
1.25	0.0064	5.2671	0.4630	1.0990	79	0.0066	5.2818	0.5364	1.0017	81
1.50	0.0067	5.6149	0.3652	0.9324	83	0.0070	5.6033	0.4391	0.8531	85
1.75	0.0075	6.3565	0.3093	0.8138	87	0.0079	6.4922	0.3667	0.7447	89
2.00	0.0071	5.9897	0.2651	0.7241	88	0.0074	6.0375	0.3173	0.6617	89
2.25	0.0079	6.7135	0.2285	0.6527	90	0.0082	6.7710	0.2757	0.5955	91
2.50	0.0080	6.8331	0.2088	0.5944	91	0.0084	6.9284	0.2503	0.5415	92
2.75	0.0110	9.6210	0.1859	0.5459	94	0.0111	9.3593	0.2229	0.4966	95
3.00	0.0111	9.6926	0.1671	0.5052	95	0.0121	10.3069	0.2037	0.4589	96
5.00	0.1537	150.8902	0.0993	0.3280	99	0.1037	98.7376	0.1204	0.2908	99
10.00	0.0023	4.2021	0.0381	0.1975	95	0.0023	4.0885	0.0439	0.1598	96
20.00	0.0001	2.5963	0.0109	0.1314	95	0.0002	2.4491	0.0133	0.0955	96
30.00	0.0014	4.9829	0.0055	0.1071	98	0.0011	4.5857	0.0064	0.0726	98
40.00	0.0013	4.0980	0.0034	0.0936	98	0.0013	4.2444	0.0039	0.0608	99

The structure's lateral stiffness $= 2K_s$

exceeding a predetermined maximum displacement. The RNC is described, modeled, characterized and subjected to extensive numerical assessment to verify its efficiency. Based on this investigation, the following conclusions can be drawn:

1. The RNC isolator is a robust isolation device and is very effective in controlling the response of motion-sensitive equipment for wide range of structural properties and earthquake characteristics.
2. The behavior of an equipment isolated by RNC isolator is relatively independent of the frequency content and the amplitude of base excitation.
3. From harmonic analysis, the results indicate that the RNC isolator is more effective in reducing the equipment acceleration response at the resonant frequency of the primary structure, while keeping the associated equipment motion below 0.30 m.
4. Under a series of 36 actual earthquakes, the maximum attained reduction in the peak absolute acceleration of equipment by the RNC isolator is 98 percent for many earthquakes, while the associated equipment-floor relative displacement is always affordable.
5. Under long-period ground motions like the Mexico City earthquake, the isolation of the entire housing structure is not the convenient approach to protect equipment, contrary to the RNC-isolated raised floor, which can eliminate up to 67 percent of the equipment acceleration.
6. Excluding the long period ground motions, the direct isolation of equipment via RNC-isolated raised-floor system is far superior to the isolation of the entire housing structure using RNC isolators. Anyway, the equipment acceleration is significantly reduced using both approaches.
7. Increasing the isolated equipment mass (reducing its frequency) increases the rolling displacement but reduces the equipment acceleration. On the other hand, the variation of the structural stiffness has a minimal influence on the response of the isolated equipment.

Acknowledgments

The first author acknowledges the support of the Generalitat de Catalunya through the FI fellowship program. The support of the patent office in the Technical University of Catalonia (UPC) is deeply appreciated. This work has been performed under the Project DPI 2005-08668-C03-01 sponsored by the Ministry of Science and Innovations of Spain.

References

[1] J.S. Hwang, Y.N. Huang, Y.H. Hung, J.C. Huang, Applicability of seismic protective systems to structures with vibration-sensitive equipment, *Journal of Structural Engineering, ASCE* 130 (11) (2004) 1676–1684.

[2] L.Y. Lu, G.L. Lin, Predictive control of smart isolation system for precision equipment subjected to near-fault earthquakes, *Engineering Structures* 30 (2008) 3045–3064.
[3] M. Hamidi, M.H. El Naggar, On the performance of SCF in seismic isolation of the interior equipment of buildings, *Earthquake Engineering and Structural Dynamics* 36 (2007) 1581–1604.
[4] F. Naeim, J.M. Kelly, *Design of Seismic Isolated Structures—from Theory to Practice*, Wiley, New York, 1999.
[5] G.F. Demetriades, M.C. Constantinou, A.M. Reinhorn, Study of wire rope systems for seismic protection of equipment in buildings, *Engineering Structures* 15 (5) (1993) 321–334.
[6] V. Lambrou, M.C. Constantinou, Study of seismic isolation systems for computer floors, Technical Report, NCEER-94-0020, July, 1994.
[7] A. Kasalanati, A.M. Reinhorn, M.C. Constantinou, D. Sanders, Experimental study of ball-in-cone isolation system, *Proceedings of the ASCE Structures Congress XV*, April 13–16, 1997, pp. 1191–1195.
[8] B. Myslimaj, S. Gamble, D. Chin-Quee, A. Davies, Base isolation technologies for seismic protection of museum artifacts, *The 2003 IAMFA Annual Conference in San Francisco*, California, September 21–24, 2003.
[9] L.Y. Lu, Y.B. Yang, Dynamic response of equipment in structures with sliding support, *Earthquake Engineering and Structural Dynamics* 26 (1997) 61–77.
[10] T.M. Al-Hussaini, V.A. Zayas, M.C. Constantinou, Seismic isolation of a multi-story frame structure using spherical sliding isolation systems, Technical Report, NCEER-94-0007, National Center of Earthquake Engineering Research, Buffalo, NY, 1994.
[11] M. Hamidi, M.H. El Naggar, A. Vafai, G. Ahmadi, Seismic isolation of buildings with sliding concave foundation (SCF), *Earthquake Engineering and Structural Dynamics* 32 (2003) 15–29.
[12] T.W. Lin, C.C. Hone, Base isolation by free rolling rods under basement, *Earthquake Engineering and Structural Dynamics* 22 (1993) 261–273.
[13] T.W. Lin, C.C. Chern, C.C. Hone, Experimental study of base isolation by free rolling rods, *Earthquake Engineering and Structural Dynamics* 24 (1995) 1645–1650.
[14] R.S. Jangid, Stochastic seismic response of structure isolated by rolling rods, *Engineering Structures* 22 (2000) 937–946.
[15] R.S. Jangid, Y.B. Londhe, Effectiveness of elliptical rolling rods for base isolation, *Journal of Structural Engineering, ASCE* 124 (1998) 469–472.
[16] Q. Zhou, X. Lu, Q. Wang, D. Feng, Q. Yao, Dynamic analysis on structures base-isolated by a ball system with restoring property, *Earthquake Engineering and Structural Dynamics* 27 (1998) 773–791.
[17] H.P. Gavin, A. Zaicenco, Performance and reliability of semi-active equipment isolation, *Journal of Sound and Vibration* 306 (2007) 74–90.
[18] J.M. Kelly, Seismic isolation of civil buildings in the USA, *Progress in Structural Engineering and Materials* 3 (1998) 279–285.
[19] P. Murnal, R. Sinha, Aseismic design of structure–equipment systems using variable frequency pendulum isolator, *Nuclear Engineering and Design* 231 (2004) 129–139.
[20] D.M. Fenz, M.C. Constantinou, Spherical sliding isolation bearings with adaptive behavior: theory, *Earthquake Engineering and Structural Dynamics* 37 (2008) 163–183.
[21] D.M. Fenz, M.C. Constantinou, Spherical sliding isolation bearings with adaptive behavior: experimental verification, *Earthquake Engineering and Structural Dynamics* 37 (2008) 185–205.
[22] Y.L. Xu, Z.F. Yu, S. Zhan, Experimental study of a hybrid platform for high-tech equipment protection against earthquake and microvibration, *Earthquake Engineering and Structural Dynamics* 37 (2008) 747–767.
[23] Y.L. Xu, B. Li, Hybrid platform for high-tech equipment protection against earthquake and microvibration, *Earthquake Engineering and Structural Dynamics* 35 (2006) 943–967.
[24] Y.L. Xu, H.J. Liu, Z.C. Yang, Hybrid platform for vibration control of high-tech equipment in buildings subject to ground motion. Part 1: experiment, *Earthquake Engineering and Structural Dynamics* 32 (2003) 1185–1200.
[25] Z.C. Yang, Y.L. Xu, J. Chen, H.J. Liu, Hybrid platform for vibration control of high-tech equipment in buildings subject to ground motion. Part 2: analysis, *Earthquake Engineering and Structural Dynamics* 32 (2003) 1201–1215.
[26] Y.C. Fan, C.H. Loh, J.N. Yang, P.Y. Lin, Experimental performance evaluation of an equipment isolation using MR dampers, *Earthquake Engineering and Structural Dynamics* 38 (3) (2008) 285–305.
[27] C. Alhan, H.P. Gavin, Reliability of base isolation for the protection of critical equipment from earthquake hazards, *Engineering Structures* 27 (2005) 1435–1449.
[28] M. Ismail, J. Rodellar, F. Ikhouane, A seismic isolation system for supported objects, Patent Number P200802043, Spanish Office of Patents and Marks, 2008.
[29] ANSYS release 11 documentation, ANSYS, Inc. Southpointe, 275 Technology Drive, Canonsburg, PA, 2008.
[30] *AASHTO LRFD Bridge Design Specifications*, *SI Units*, third ed., American Association of State Highway and Transportation Officials, 2005, Interim Revisions Washington DC, 20001, USA.
[31] Y.K. Wen, Method for random vibration of hysteretic systems, *Journal of the Engineering Mechanics Division* 102 (EM2) (1976) 246–263.
[32] F. Ikhouane, J. Rodellar, On the hysteretic Bouc–Wen model. Part I: forced limit cycle characterization, *Nonlinear Dynamics* 42 (2005) 63–78.
[33] F. Ikhouane, J. Rodellar, On the hysteretic Bouc–Wen model. Part II: robust parametric identification, *Nonlinear Dynamics* 42 (2005) 79–95.
[34] F. Ikhouane, O. Gomis-Bellmunt, A limit cycle approach for the parametric identification of hysteretic systems, *Systems & Control Letters* 57 (2008) 663–669.
[35] F. Ikhouane, V. Mañosa, J. Rodellar, Dynamic properties of the hysteretic Bouc–Wen model, *Systems and Control Letters* 56 (2007) 197–205.
[36] C.M. Uang, V.V. Bertero, Evaluation of seismic energy in structures, *Earthquake Engineering and Structural Dynamics* 19 (1990) 77–90.
[37] SAP2000 release 11 documentation, Computer and Structure, Inc., 1995 University Ave, Berkeley, CA, 2008.
[38] E.L. Wilson, *Three-Dimensional Static and Dynamic Analysis of Structures*, third ed., CSI, Computers and Structures, Inc., Berkeley, CA, USA, 2002.